# Prediction of Phosphorus Sorption Index and Availability by NIR and MIR in Soils in Madagascar

Henintsoa V. Ramaroson [1,2] , Thierry Becquer [3,*] , Hery Razafimahatratra [2,4] , Ando Razakavololona [1], Lilia Rabeharisoa [2,4] and Amos F. M. Rakotondrazafy [5]

1    Ecole Normale Supérieure d'Ampefiloha, Université d'Antananarivo, Antananarivo 101, Madagascar
2    Laboratoire des RadioIsotopes, Université d'Antananarivo, Route d'Andraisoro, Antananarivo 101, Madagascar
3    Eco&Sols, IRD, INRAE, CIRAD, L'Institut Agro Montpellier, Université Montpellier, 34060 Montpellier, France
4    Ecole Supérieure des Sciences Agronomiques, Université d'Antananarivo, Antananarivo 101, Madagascar
5    Faculté des Sciences, Université d'Antananarivo, Antananarivo 101, Madagascar
*    Correspondence: thierry.becquer@ird.fr

**Abstract:** The development of techniques for the rapid, inexpensive, and accurate determination of the phosphorus (P) availability and sorption index (PSI) in soils is important for P management in highly weathered tropical soils. The applicability of near- and mid-infrared reflectance spectroscopy (NIR and MIR) as tools for estimating P availability and PSI was assessed over a wide range of highly weathered soils in Madagascar. The predictions were based on chemometric methods using multi-variate calibration models with partial least squares (PLS) regressions, and pedotransfer functions (PTFs). Chemometric methods failed to predict available P ($P_{resin}$). However, a P sorption index, determined as the P remaining in solution ($P_{rem}$), was estimated with acceptable accuracy with both NIR and MIR ($R^2_{cv} = 0.70 - 0.73$; $R^2_v = 0.65 - 0.77$; SEP(c) = $5.5 - 4.6$ mg kg$^{-1}$). The PTFs showed that the PSI was well explained by iron oxide, gibbsite, and sand contents, all of these compounds being well predicted by NIR or MIR ($R^2_v > 0.70$). These results indicate that NIR and MIR can be helpful for a rapid estimate of PSI of highly weathered ferralitic soils.

**Keywords:** diffuse reflectance spectroscopy; chemometrics; pedotransfer functions; phosphorus sorption; soil mineral composition; highly weathered tropical soils

## 1. Introduction

Phosphorus (P) is one of the main growth-limiting nutrients for plants. The lack of adequate levels of available P in soils is one of the major constraints for crop production in tropical soils, e.g., in Madagascar [1]. Consequently, crop yields remain low and far below their potential. Soil P deficiency may be due to the low P-status of the parent material, soil weathering, mismanagement through imbalance between nutrient input and export by harvested products and loss of P, e.g., through soil erosion. Moreover, many tropical soils are marked by a high P-fixing capacity. These soils have a predominance of 1:1 clay minerals, such as kaolinite, iron (Fe), and aluminum (Al) oxides. These minerals have a particularly strong affinity for the phosphate ion [2,3]. Whereas the demand for P is predicted to increase by 50–100% by 2050 to meet increasing nutritional demand, phosphate reserves will be depleted in 50–100 years [4]. Although this pessimistic view is not shared by all [5], corrective fertilization of soils with large amounts of phosphate fertilizers is not feasible in most African countries. Thus, improving P use efficiency in highly weathered P-sorbing tropical soils is of great concern.

There are a number of standard chemical methods for the determination of available soil P (e.g., Bray, Mehlich, Olsen; see [6], and references cited therein). Depending on soil types or previous fertilization history, these indexes often fail to satisfactorily predict P availability [7]. In fact, these chemical methods dissolve P-forms not readily available for plants in proportions that vary with the nature and duration of the extraction, the type of

soil, and the history of fertilization [8]. However, in many countries, recommendations for fertilizer P application are based on such P availability index. Phosphorus sorption or desorption methods have also been used for measuring fast and reversible P sorption [9]. As the soil solution only contains about 1% of the uptake by the crop, this means that 99% of the P is replenished from the solid constituents of the soil. So, according to Barrow [10], the measurement of adsorption/desorption is also useful to predict the amount of fertilizer needed for plant growth. In acidic soils, the Al and Fe minerals are key constituents of sorption processes. Desorption of soil P by anion-exchange resins mimics the process of P uptake by plant roots, which makes this method one of the most applied methods to assess plant-available P [9]. The P sorption in soils has traditionally been evaluated by the P buffer capacity (PBC; [11]), i.e., determined as the slope of the P sorption curve, which provides a useful tool for improved management of P in agricultural systems [12,13]. A simple, single-addition P-sorption index (PSI) was successfully developed as a surrogate of PBC in Australian and Brazilian soils [14,15].

For a few years, near- and mid-infrared spectrometry (NIR, in the wavelength range 1100–2500 nm, and MIR, in the wavelength range 2500–25,000 nm) have been used extensively for the prediction of various soil properties [16–18]. Various studies focus on the determination of the potentially available P fractions or on the ability of soil to bind P (P sorption). With a few exceptions of soil sets representing special or unusual conditions, most predictions of extractable P in soils resulted either in low $R^2$ values (0.5–0.7) for calibration or were considered to be completely unreliable ($R^2 < 0.50$) [18,19]. However, some successful models for South African and Australian soils were reported for PBI by using NIR or MIR spectroscopy, with prediction $R^2$ values ranging from 0.69 to 0.87 for calibration (see [20]). Recent results also showed the potential of MIR spectrometry to predict PSI for temperate soils [21]. Success in predictions of P sorption by infrared spectroscopy may be attributed to the response of the infrared spectra to the soil components in the soil matrix that present a great affinity for phosphate anions (i.e., some minerals such as Al- and Fe-oxyhydroxides and carbonates, SOM/Al complexes) [18].

According to Minasny et al. [22], P adsorption capacity can be predicted from clay content, pH, and soil color, using pedotransfer function (PTF), i.e., a relationship between soil parameters and the easier measurable properties usually available from routine soil analysis. Aluminum and iron oxide fractions, such as oxalate-extractable aluminum and iron and dithionite-extractable iron [23], have also been found to be useful predictors. As the predictions of soil minerals using spectral methods have been found to be effective in highly weathered tropical soils [24,25], NIR and MIR spectrometry can be useful tools to predict some of the mineralogical properties of the soils and use them in PTF.

The main objective of this study was to investigate the use of NIR and MIR spectroscopy to predict the desorption of soil P, using anion-exchange resins ($P_{resin}$), and sorption of soil P, using single-addition P-sorption index (PSI), over a wide range of highly weathered soils in Madagascar. We also built pedotransfer functions for predicting PSI and compared the usefulness of applying spectrally predicted soil parameters in the PTFs, that could be used as a complementary tool to standard chemical methods.

## 2. Materials and Methods

### 2.1. Soil Sampling and Analysis

A set of Malagasy soils, described in a previous study [25], was used for this study. Briefly, highly weathered soils, classified as Ferralsols, Cambisols, and Nitisols [26], were collected at 120 sites in Madagascar (Figure 1). At each site, composite samples were taken at 0–0.1, 0.1–0.2, 0.2–0.3, 0.5–0.6, and 0.8–0.9 m depth, resulting in 600 soil samples.
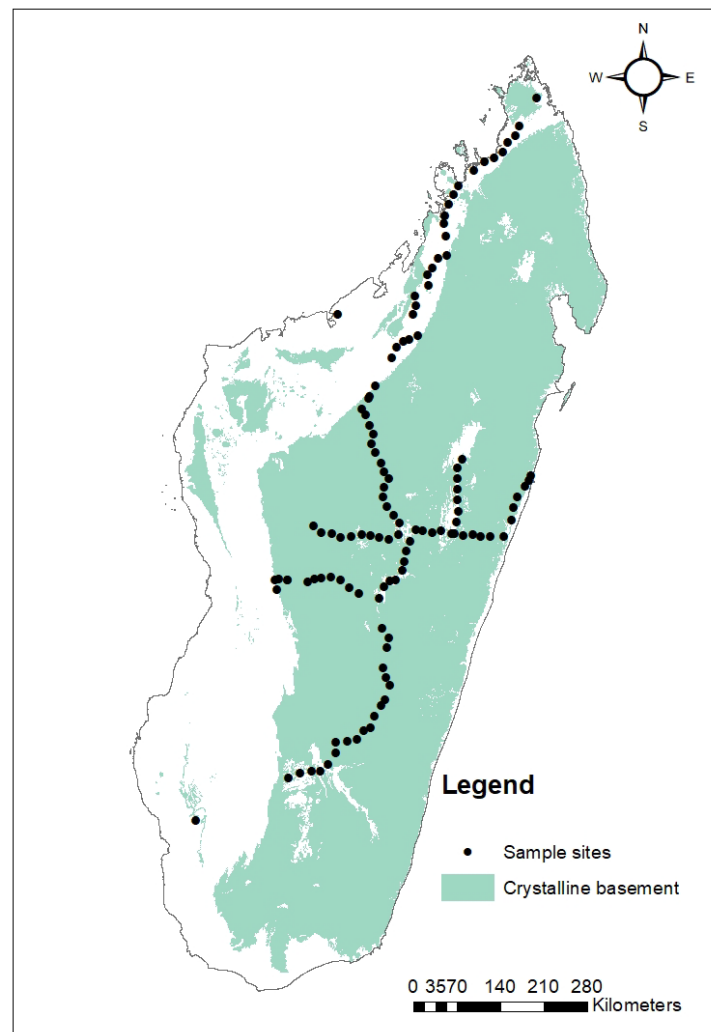
**Figure 1.** Sampling site location in Madagascar.

The spectra of the 600 samples were acquired, and 148 of those were selected from all the five soil horizons, according to their NIR spectral representativeness, and analyzed by reference methods.

For $P_{resin}$ extraction, one 6 cm$^2$ strip of anion exchange membrane in bicarbonate form (Product 55164 2S; BDH Laboratory Supplies, Poole, England, anion exchange capacity: 0.037 $cmol_c$ $cm^{-2}$) was shaken with 2 g of soil and 30 mL of deionized water on an end-over-end shaker at 25 °C for 16 h. The resin strip was removed and washed. The phosphate extracted by the resin was eluted by shaking for 30 min with 30 mL 0.1 M NaCl/0.1 M HCl. The PSI was determined after a single addition of 60 mg P $L^{-1}$ (as $KH_2PO_4$) in 0.01M $CaCl_2$ added at a 1:10 soil:solution ratio [27]. The suspensions were equilibrated by shaking in an end-over-end shaker at 25 °C for 16 h. After equilibrium, P remaining in solution ($P_{rem}$) was determined. Total soil P ($P_{total}$) was determined after digestion of 0.1 g of soil with 2 mL $HClO_4$ at 205 °C for 2 h. The extracted orthophosphate was determined spectrophotometrically using the blue molybdate-ascorbic acid method.

Total C was analyzed by dry combustion in a LECO model CHN 600 (Leco Corp., St Joseph, MI, USA). The soil pH was measured in distilled water ($pH_{water}$) using a 1:2.5 (mass) soil:solution ratio. The particle size distribution was determined with the pipette method after dispersing with 1 M NaOH.

Iron oxides were dissolved using the citrate-bicarbonate-dithionite (CBD) deferrification method of Mehra and Jackson [28]. The $Fe_2O_{3cbd}$ content represents the amount of free iron oxide components of soils. The kaolinite (Kt), gibbsite (Gb), goethite (Gt), and

hematite (Hm) contents were computed according to the methodology of Reatto et al. [29] after digestion with sulphuric acid (SA) (1:1 distilled water/conc. $H_2SO_4$ volume ratio) (see [24,25,29], for details).

### 2.2. NIR and MIR Spectrometry

The reflectance of the soil samples was determined in the near-infrared region using a Foss NIRSystems 5000 spectrophotometer (Silver Spring, MD, USA) and in the mid-infrared region using a Nicolet 6700 spectrophotometer (Thermo Fisher Scientific Instruments, Madison, WI, USA). For NIR spectrometry, approximately 5 g of finely ground soil (<200 µm), packed into a 5 cm diameter ring cup with a quartz window, was scanned in the 1100 to 2498 nm range with a resolution of 2 nm. MIR analyses were subsequently performed on the same samples. The reflectance was measured over the range of 400–4000 $cm^{-1}$ (2500–25,000 nm) with a spectral resolution of 3.86 $cm^{-1}$. Each sample spectrum was averaged from 15 spectra for NIR and 25 for MIR. Data were analyzed using the WinISI III–V 1.63e software (Foss NIR Systems/TecatorInfrasoft International, LLC, Silver Spring, MD, USA).

Among the 148 representative samples, we used PCAs (principal component analysis) to look for the best cluster of data and to select independently the sets of calibration and validation for NIR and MIR. The best PCAs were calculated using SNVD 2441 for NIR and SNVD 0441 for MIR. This resulted in different calibration and validation sets for NIR and MIR, with, respectively, 104 and 42 samples (2 outliers) for calibration and validation sets for NIR, and 104 and 41 samples (3 outliers) for calibration and validation sets for MIR. NIR and MIR multivariate calibration models were performed as described previously [25], using modified partial least squares regression (mPLS). The spectral pre-processing techniques used included no pre-processing (NONE), multiplicative scatter correction (MSC), standard normal variate (SNV), detrending (DETREND), and SNV with detrending (SNVD). The four successive numbers corresponded to the derivatives (0, 1, and 2: no derivation, first and second derivatives, respectively), the number of point gaps (0, 4, 5, 10), the number of points for first smoothing (1, 4, 5, 10), and the number of points for second smoothing (always 1). The mPLS regression was achieved using 15 and 25 mPLS factors for NIR and MIR, respectively. The numbers of mPLS factors were determined by minimizing the standard error of cross-validation over the calibration sets.

The performance of the calibration model was assessed using the coefficient of determination of cross-validation ($R^2_{cv}$) and the ratio of performance to deviation ($RPD_{cv}$), which is the ratio of standard deviation to the standard error of cross-validation (SECV), and was considered acceptable for $RPD_{cv} > 2$, and $R^2_{cv} > 0.75$ [30,31]. The prediction accuracy of the model was evaluated on the validation subset (which had not been used for model development), using the validation $R^2_v$ and $RPD_v$.

We analyzed the kaolinite and gibbsite by specific diagnostic absorption peaks in the NIR range at around 2205 nm for kaolinite and 2265 nm for gibbsite [25,32]. Data processing was performed by R software with packages xlsx, car, FacToMineR, lattice, Mass, leaps, Hmisc et ade4 [25].

### 2.3. Calibration of Pedotransfer Functions

Pedotransfer functions were built for the prediction of $P_{resin}$ and $P_{rem}$ as a function of mineralogical and physico-chemical soil properties. Stepwise multiple linear regression analysis was carried out with the R software with packages xlsx, car, FacToMineR, lattice, Mass, leaps, Hmisc et ade4 for establishing a function in which $P_{resin}$ or $P_{rem}$ were dependent variables on the other determined soil properties as independent variables. PTF models were built to relate $P_{resin}$ and $P_{rem}$ (i) to the chemically measured mineralogical (Kt, Gb, $Fe_2O_{3cbd}$) and physico-chemical ($pH_{water}$, C, clay, silt, sand) covariates and (ii) to the mineralogical and physico-chemical covariates predicted by NIR or MIR spectrometry (all except $pH_{water}$).

## 3. Results

### 3.1. Reference Soil Analysis

The mean values, standard deviation, and variation range are shown in Table 1 for mineralogical characteristics, particle size distribution, and chemical characteristics of the soils. A large variability was observed in the studied soils. Kaolinite was the dominant mineral of the clay fraction ($305 \pm 148$ g kg$^{-1}$) followed by gibbsite ($110 \pm 117$ g kg$^{-1}$) (Table 1). Crystalline iron oxides, estimated by CBD extraction (Fe$_2$O$_{3cbd}$), amounted to $42 \pm 31$ g kg$^{-1}$. The most common textural classes among all soil samples were coarse-loam to clay. The clay content ranged from 1 to 766 g kg$^{-1}$ with a mean of $332 \pm 151$ g kg$^{-1}$. The silt and sand means were $216 \pm 122$ and $451 \pm 199$ g kg$^{-1}$, respectively. These values are quite similar to those of Grinand et al. [33] who found 300, 161, and 517 g kg$^{-1}$ for clay, silt, and sand, respectively, for a large database (618 samples) of soils from Madagascar. The total C content of the soils varied from 1.2 to 85.5 g kg$^{-1}$, with mean values of $14.0 \pm 12.9$ g kg$^{-1}$, also very close to those of Grinand et al. [33], i.e., $11.8 \pm 7.2$ g kg$^{-1}$. The soils were generally acidic, with a mean pH$_{water}$ of $5.5 \pm 0.6$.

**Table 1.** Summary statistics for constituents and physico-chemical properties of the ferrallitic soils studied.

| Constituent | Unit | Min | Max | Mean | SD | Median |
|---|---|---|---|---|---|---|
| Kt [1] | g kg$^{-1}$ | 13.3 | 676.3 | 304.7 | 147.9 | 288.3 |
| Gb [2] | g kg$^{-1}$ | 0.0 | 456.2 | 109.9 | 116.9 | 83.8 |
| Fe$_2$O$_{3cbd}$ [3] | g kg$^{-1}$ | 0.0 | 181.4 | 42.4 | 30.5 | 37.2 |
| Clay | g kg$^{-1}$ | 1.4 | 766.1 | 332.1 | 151.0 | 342 |
| Silt | g kg$^{-1}$ | 20.2 | 566.0 | 216.3 | 122 | 188 |
| Sand | g kg$^{-1}$ | 42.6 | 901.6 | 451.6 | 199.1 | 442.8 |
| C [4] | g kg$^{-1}$ | 1.2 | 85.5 | 14.0 | 12.9 | 10.2 |
| pH$_{water}$ | | 2.4 | 7.1 | 5.5 | 0.6 | 5.5 |
| P$_{tot}$ [5] | mg kg$^{-1}$ | 12.7 | 1955.4 | 374.3 | 318.5 | 259.6 |
| P$_{resin}$ [6] | mg kg$^{-1}$ | 0.0 | 4.4 | 0.8 | 0.9 | 0.4 |
| P$_{rem}$ [7] | mg kg$^{-1}$ | 1.2 | 47.4 | 23.1 | 9.5 | 22.8 |

[1] Kaolinite; [2] gibbsite; [3] amount of Fe determined by the CBD method; [4] carbon; [5] phosphorus total; [6] phosphorus available; [7] phosphorus remaining in solution.

The total (P$_{total}$), available (P$_{resin}$), and remaining (P$_{rem}$) P contents varied considerably among samples (Table 1), with ranges of 13–1955, 0–4.4, and 1.2–47.4 g kg$^{-1}$, respectively. The means for P$_{tot}$, P$_{resin}$, and P$_{rem}$ were $374 \pm 319$, $0.8 \pm 0.9$, and $23.1 \pm 9.5$ mg kg$^{-1}$, respectively. The low availability of P (P$_{resin}$) is similar to that observed in other soils [1] and explains the P deficiencies generally observed in soils of the Highlands in Madagascar [34].

### 3.2. NIR and MIR Prediction of Soil Variables through Chemometric Approach

Prediction of soil phosphorus using both NIR and MIR spectrometry based on multivariate regression through principal components and partial least squares approaches were poorly effective (Table 2). Only P$_{rem}$ was satisfactorily calibrated, according to the classification of Chang et al. [30] and Malley et al. [31], with $R^2_{cv} = 0.70$ and 0.73, and RPD$_{cv} = 1.8$ and 1.9, respectively, for NIR and MIR spectrometry. The $R^2_v$ were similar (0.65–0.77), with SEP(c) = 5.5–4.6) making it usable for prediction. The predictions of P$_{resin}$ and P$_{tot}$ were unsatisfactory ($R^2_v < 0.40$).

**Table 2.** Calibration and validation statistics of soil phosphorus properties, using NIR and MIR.

| Constituent | Unit | Preprocessing | N [6] | Out [7] | n1 [8] | Mean | SD [9] | SECV [10] | $R^2_{cv}$ [11] | $RPD_c$ [12] |
|---|---|---|---|---|---|---|---|---|---|---|
| **Calibration Set** | | | | | | | | | | |
| NIR | | | | | | | | | | |
| $P_{tot}$ [1] | mg kg$^{-1}$ | None [4] 2441 * | 104 | 4 | 100 | 318.8 | 230.8 | 193.5 | 0.30 | 1.2 |
| $P_{resin}$ [2] | mg kg$^{-1}$ | None 1441 * | 104 | 5 | 99 | 0.8 | 0.9 | 0.6 | 0.56 | 1.5 |
| $P_{rem}$ [3] | mg kg$^{-1}$ | None 1441 | 104 | 4 | 100 | 24.0 | 9.1 | 5.0 | 0.70 | 1.8 |
| MIR | | | | | | | | | | |
| $P_{tot}$ [1] | mg kg$^{-1}$ | None 1441 | 104 | 6 | 98 | 352.3 | 256.4 | 167.0 | 0.57 | 1.5 |
| $P_{resin}$ [2] | mg kg$^{-1}$ | Snvd [5] 1441 | 104 | 8 | 96 | 0.7 | 0.8 | 0.6 | 0.43 | 1.3 |
| $P_{rem}$ [3] | mg kg$^{-1}$ | Snvd 0011 * | 104 | 3 | 101 | 23.3 | 9.5 | 5.0 | 0.73 | 1.9 |

| Constituent | Unit | Preprocessing | n2 [13] | Mean | SD | SEP(c) [14] | Bias | Slope | $R^2_v$ [15] | $RPDv$ [16] |
|---|---|---|---|---|---|---|---|---|---|---|
| **Validation Set** | | | | | | | | | | |
| NIR | | | | | | | | | | |
| $P_{tot}$ [1] | mg kg$^{-1}$ | None 2441 | 42 | 321.2 | 136.2 | 261.9 | 34.5 | 1.1 | 0.26 | 1.2 |
| $P_{resin}$ [2] | mg kg$^{-1}$ | None 1441 | 42 | 0.8 | 0.8 | 3.8 | 0.4 | 0.5 | 0.01 | 1.0 |
| $P_{rem}$ [3] | mg kg$^{-1}$ | None 1441 | 42 | 24.0 | 8.0 | 5.5 | −0.4 | 0.9 | 0.65 | 1.7 |
| MIR | | | | | | | | | | |
| $P_{tot}$ [1] | mg kg$^{-1}$ | None 1441 | 41 | 366.84 | 255.5 | 210.1 | 23.3 | 1.0 | 0.60 | 1.6 |
| $P_{resin}$ [2] | mg kg$^{-1}$ | Snv 1441 | 41 | 0.7 | 0.8 | 7.1 | 1.0 | 1.0 | 0.0.1 | 1.0 |
| $P_{rem}$ [3] | mg kg$^{-1}$ | Snvd 0011 | 41 | 23.2 | 8.5 | 4.6 | −0.1 | 1.0 | 0.77 | 2.1 |

[1] Total phosphorus; [2] phosphorus available; [3] phosphorus remaining in solution; [4] no preprocessing; [5] standard normal variate and detrend; * the numbers indicate the derivatives (0, 1, and 2: no derivation, first and second derivatives, respectively)—number of point gap (0, 4)—number of points for first smoothing (1, 4) and number of points for second smoothing (1); [6] total number of sample; [7] number of outliers; [8] number of samples in the calibration set (N—out); [9] standard deviation; [10] standard error of cross-validation; [11] coefficient of determination of cross-validation that corresponds to the percent of variation described in the data; [12] ratio performance deviation of cross-validation (SD/SECV); [13] number of samples in the validation set; [14] standard error of prediction corrected; [15] coefficient of determination of SEP; [16] 1/[racine (1 − $R^2$)].

Calibration and validation statistics of physico-chemical and mineralogical soil properties, using mPLS methods on NIR and MIR spectra, were presented in Table 3. The accuracies of the prediction of the carbon content of the soils were considered successful using NIR ($R^2_{cv}$ = 0.79 and $RPD_{cv}$ = 2.1) and excellent using MIR ($R^2_{cv}$ = 0.85 and $RPD_{cv}$ = 2.6). For mineralogy and texture, most of the predictions resulted in lower $R^2$ values (0.5–0.7), for both NIR and MIR. The best predictions were obtained for $Fe_2O_{3cbd}$ with NIR ($R^2_{cv}$ = 0.80 and $RPD_{cv}$ = 2.2) and sand ($R^2_{cv}$ = 0.66 and $RPD_{cv}$ = 1.7) with MIR. The prediction of the main minerals of the soils, i.e., kaolinite and gibbsite, had $R^2_c$ values between 0.5–0.6 and $R^2_v$ still lower. However, in a previous paper on the same soils [25], we got satisfactory coefficients of determination for gibbsite and kaolinite, with adjusted $R^2_{cv}$ = 0.71 and 0.69, respectively, and similar results for the calibration set, using the height of the second derivative of NIR specific spectral peaks situated at nearly 2205 nm for kaolinite and 2265 nm for gibbsite. The pH$_{water}$ predictions were completely unreliable ($R^2_{cv}$ < 0.40) (Table 3).

**Table 3.** Calibration and validation statistics of physico-chemical and mineralogical soil properties, using NIR and MIR.

| Constituent | Unit | Preprocessing | Calibration Set | | | | | | | |
|---|---|---|---|---|---|---|---|---|---|---|
| | | | N [10] | Out [11] | n1 [12] | Mean | SD [13] | SECV [14] | $R^2_{cv}$ [15] | $RPD_{cv}$ [16] |
| NIR | | | | | | | | | | |
| Kt [1] | g kg$^{-1}$ | None [5] 2441 * | 104 | 5 | 99 | 309.3 | 147.8 | 95.0 | 0.60 | 1.6 |
| Gb [2] | g kg$^{-1}$ | None 0011 * | 104 | 34 | 70 | 138.4 | 107.07 | 67.8 | 0.60 | 1.6 |
| Fe$_2$O$_{3cbd}$ [3] | g kg$^{-1}$ | Msc [6] 2551 * | 104 | 9 | 95 | 36.9 | 26.0 | 11.8 | 0.80 | 2.2 |
| C [4] | g kg$^{-1}$ | None 1441 * | 104 | 4 | 100 | 1.3 | 1.1 | 0.5 | 0.79 | 2.1 |
| Clay | g kg$^{-1}$ | None 0011 * | 104 | 4 | 100 | 311.4 | 136.4 | 97.7 | 0.49 | 1.4 |
| Silt | g kg$^{-1}$ | Snv [7] 1441 * | 104 | 3 | 101 | 211.0 | 127.2 | 99.0 | 0.39 | 1.3 |
| Sand | g kg$^{-1}$ | Snv 1441 | 104 | 4 | 100 | 480.1 | 196.3 | 127.9 | 0.58 | 1.5 |
| pH$_{water}$ | | Snv 2441 * | 104 | 4 | 100 | 5.46 | 0.4 | 0.3 | 0.37 | 1.3 |
| MIR | | | | | | | | | | |
| Kt | g kg$^{-1}$ | None 0011 | 104 | 6 | 98 | 298.9 | 140.1 | 90.3 | 0.59 | 1..6 |
| Gb | g kg$^{-1}$ | None 0011 | 104 | 25 | 79 | 149.4 | 116.2 | 78.4 | 0.54 | 1.5 |
| Fe$_2$O$_{3cbd}$ | g kg$^{-1}$ | Detrend [8] 1441 | 104 | 6 | 98 | 40.9 | 25.6 | 16.7 | 0.57 | 1.5 |
| C | g kg$^{-1}$ | Snvd [9] 1441 | 104 | 7 | 97 | 1.1 | 0.9 | 0.3 | 0.85 | 2.6 |
| Clay | g kg$^{-1}$ | Snv 210101 * | 104 | 6 | 98 | 349.4 | 131.1 | 87.3 | 0.56 | 1.5 |
| Silt | g kg$^{-1}$ | Snv 2551 | 104 | 4 | 100 | 218.2 | 116.6 | 76.5 | 0.58 | 1.5 |
| Sand | g kg$^{-1}$ | Snv 0011 | 104 | 2 | 102 | 441.2 | 186.9 | 110.0 | 0.66 | 1.7 |
| pH$_{water}$ | | Snvd 0011 | 104 | 7 | 97 | 5.5 | 0.4 | 0.4 | 0.24 | 1.1 |

| Constituent | Unit | Preprocessing | Validation Set | | | | | | | |
|---|---|---|---|---|---|---|---|---|---|---|
| | | | n2 [17] | Mean | SD | SEP(c) [18] | Bias | Slope | $R^2_{v}$ [19] | $RPD_{v}$ [20] |
| NIR | | | | | | | | | | |
| Kt | g kg$^{-1}$ | None 2441 | 42 | 301.2 | 127.1 | 125.5 | −28.0 | 0.7 | 0.37 | 1.3 |
| Gb | g kg$^{-1}$ | None 0011 | 42 | 184.3 | 92.9 | 83.5 | 10.5 | 0.9 | 0.51 | 1.4 |
| Fe$_2$O$_{3cbd}$ | g kg$^{-1}$ | Msc 2551 | 42 | 52.3 | 27.2 | 21.3 | 1.4 | 1.0 | 0.63 | 1.6 |
| C | g kg$^{-1}$ | none 1441 | 42 | 1.5 | 0.8 | 0.4 | −0.2 | 0.9 | 0.81 | 2.3 |
| Clay | g kg$^{-1}$ | None 0011 | 42 | 348.4 | 74.6 | 114.6 | 49.3 | 1.1 | 0.33 | 1.2 |
| Silt | g kg$^{-1}$ | Snv 1441 | 42 | 226.8 | 99.9 | 132.4 | −18.8 | 0.1 | 0.02 | 1.0 |
| Sand | g kg$^{-1}$ | Snv 1441 | 42 | 431.6 | 133.1 | 143.7 | −37.3 | 0.9 | 0.40 | 1.3 |
| pH$_{water}$ | | snv 2441 | 42 | 5.5 | 0.3 | 0.7 | 0.2 | 1.5 | 0.27 | 1.2 |
| MIR | | | | | | | | | | |
| Kt | g kg$^{-1}$ | None 0011 | 41 | 312.3 | 93.1 | 126.4 | 8.5 | 0.9 | 0.30 | 1.2 |
| Gb | g kg$^{-1}$ | None 0011 | 41 | 121.5 | 78.0 | 67.8 | 11.9 | 0.8 | 0.45 | 1.3 |
| Fe$_2$O$_{3cbd}$ | g kg$^{-1}$ | Detrend 1441 | 41 | 38.9 | 24.6 | 22.5 | 5.7 | 1.4 | 0.72 | 1.9 |
| C | g kg$^{-1}$ | Snvd 1441 | 41 | 1.4 | 0.9 | 0.4 | 0.0 | 1.0 | 0.87 | 2.8 |
| Clay | g kg$^{-1}$ | Snv 210101 | 41 | 328.2 | 105.6 | 117.5 | 6.2 | 1.2 | 0.55 | 1.5 |
| Silt | g kg$^{-1}$ | Snv 2551 | 41 | 232.5 | 119.4 | 107.4 | −39.6 | 0.5 | 0.32 | 1.2 |
| Sand | g kg$^{-1}$ | Snv 0011 | 41 | 442.4 | 177.5 | 115.4 | 30.3 | 1.0 | 0.76 | 2.0 |
| pH$_{water}$ | | Snvd 0011 | 41 | 5.4 | 0.3 | 0.5 | 0.1 | 1.2 | 0.38 | 1.3 |

[1] Kaolinite; [2] gibbsite; [3] amount of Fe determined by the CBD method; [4] carbon; [5] no preprocessing; [6] multiplicative scatter correction; [7] standard normal variate; [8] removes of linear and quadratic curvature of each spectrum; [9] standard normal variate and detrend; * the numbers indicate the derivatives (0, 1, and 2: no derivation, first and second derivatives, respectively)—number of point gaps (0, 4, 5, 10)—number of points for first smoothing (1, 4, 5, 10) and number of points for second smoothing (1); [10] total number of sample; [11] number of outliers; [12] number of samples in the calibration set (N—out); [13] standard deviation; [14] standard error of cross-validation; [15] coefficient of determination of cross-validation that corresponds to the percent of variation described in the data; [16] ratio performance deviation of cross-validation (SD/SECV); [17] number of samples in the validation set; [18] standard error of prediction corrected; [19] coefficient of determination of SEP; [20] 1/[racine (1 − R$^2$)].

### 3.3. Development of a PTF for Soil Phosphorus Using other Soil Variables Prediction through Chemometric Approach

Simple regression statistics (Table 4) indicated a significant linear relationship between $P_{rem}$ and C, clay, silt, sand, $Fe_2O_{3cbd}$, and Gb, whereas $pH_{water}$ and Kt were not significantly related to $P_{rem}$. Among the different soil properties, gibbsite content was the most closely and significantly correlated with $P_{rem}$ (r = −0.59). The amount of crystallized oxides was also significantly correlated with $P_{rem}$ (r = −0.49), however, the relationship with gibbsite was better than with iron oxides. Strong relationships between $P_{rem}$ and the clay (r = −0.53) and sand (r = 0.51) contents were observed, with a negative coefficient for the former and a positive one for the latter. The clay fraction was highly correlated to gibbsite and iron oxide contents (r = 0.35 and 0.54, respectively) which also had significant negative correlations with $P_{rem}$. The sand fraction behaved opposite to the clay fraction. The C content was negatively correlated with $P_{rem}$, which was a surprising result, because organic matter is supposed to reduce phosphorus retention [35], and thus increase $P_{rem}$. Soil minerals (kaolinite, gibbsite, iron oxides) play a key role in the stabilization of organic matter [36] and thus explain the significant correlation between C and Gb (r = 0.24). The chemical reaction of the soil ($pH_{water}$) does not seem to contribute much to the sorption of P, in line with the review paper of Gérard [3], explaining that the binding capacity of Fe/Al oxides varies moderately in the pH range of Madagascar soils. Regression between $P_{resin}$ and soil properties showed that $pH_{water}$, silt, and sand contents were the only significant variables (Table 4).

**Table 4.** Pearson coefficients and significance levels for correlation between physico-chemical and mineralogical soil properties and $P_{rem}$ or $P_{resin}$ of the ferrallitic soils studied.

| Variables | Unit | $P_{rem}$ [5] (mg L$^{-1}$) | | $P_{resin}$ [6] (mg L$^{-1}$) | |
|---|---|---|---|---|---|
| | | Coefficient | Significance Level | Coefficient | Significance Level |
| Kt [1] | g kg$^{-1}$ | 0.0277 | 0.7380 | −0.050 | 0.5450 |
| Gb [2] | g kg$^{-1}$ | −0.586 | 0.0000 | −0.019 | 0.8230 |
| $Fe_2O_{3cbd}$ [3] | g kg$^{-1}$ | −0.488 | 0.0000 | −0.097 | 0.2430 |
| $pH_{water}$ | | 0.120 | 0.1470 | 0.482 | 0.0000 |
| Clay | g kg$^{-1}$ | −0.533 | 0.0000 | 0.010 | 0.9080 |
| Silt | g kg$^{-1}$ | −0.167 | 0.0423 | 0.260 | 0.0014 |
| Sand | g kg$^{-1}$ | 0.507 | 0.0000 | −0.167 | 0.0431 |
| C [4] | g kg$^{-1}$ | −0.284 | 0.0005 | −0.025 | 0.7600 |

[1] Kaolinite; [2] gibbsite; [3] amount of Fe determined by the CBD method; [4] carbon; [5] phosphorus remaining in solution; [6] phosphorus available.

The multiple regression analyses developed are presented in Table 5, and illustrated graphically in Figure 2 for $P_{rem}$. For chemically analyzed variables, the strongest multiple regression ($p < 0.0001$) for $P_{rem}$ included five factors (each significant at $p$-value = 0.05), representing $pH_{water}$, texture, and mineralogy variables (Equation (1); Figure 2a). As expected, given their P sorption capacity, Fe/Al oxides (i.e., Gb and $Fe_2O_{3cbd}$) had a major effect on $P_{rem}$. The sand content (i.e., quartz), known for not having significant sorption capacity for P, counteracted the effects of Fe/Al oxides and was useful for the accurate prediction of $P_{rem}$. The $pH_{water}$, which was not correlated with $P_{rem}$ (Table 4), was removed without a substantial reduction of the model efficiency (Equation (2)). The C content had significant contributions (Equation (1)); however, its inclusion in the model improved only the explanation of variability marginally (Equation (3); Figure 2b), presumably, because of the collinearity of C with Al oxides (r = 0.24). The root-mean-square error (RMSE) was between 6.5 and 6.9 mg L$^{-1}$, depending on the models. A multiple regression equation was also obtained for $P_{resin}$ ($R^2 = 0.42$, Equation (4)) using the same five factors as for $P_{rem}$, but the efficiency of the model was greatly reduced after removing $pH_{water}$ and C content ($R^2 = 0.05$, Equation (5)). The goodness of fit of multiple regressions was lower for $P_{resin}$ than for $P_{rem}$ (Table 5).

**Table 5.** Best-fit multiple regression analyses for $P_{rem}$ or $P_{resin}$ of the ferrallitic soils studied using chemically analyzed or values predicted using spectrometry (except pH).

| Variables | Multiple Regression Equation | | $R^2{}_c$ | RMSE |
|---|---|---|---|---|
| | *Chemically analyzed variables* | | | |
| $P_{rem}$ | $P_{rem} = 22.32 + 1.55\ pH_{water} - 0.127\ C - 0.009\ Kt - 0.039\ Gb - 0.065\ Fe_2O_{3cbd} + 0.008\ S$ | (1) | 0.52 | 6.49 |
| | $P_{rem} = 25.78 - 0.13\ C - 0.031\ Gb - 0.062\ Fe_2O_{3cbd} + 0.012\ S$ | (2) | 0.49 | 6.69 |
| | $P_{rem} = 25.61 - 0.035\ Gb - 0.072\ Fe_2O_{3cbd} + 0.010\ S$ | (3) | 0.46 | 6.89 |
| $P_{resin}$ | $P_{res} = -0.208 + 0.053\ C - 0.001\ Gb + 0.001\ S$ | (4) | 0.42 | 0.70 |
| | $P_{res} = 0.284 + 0.001\ S$ | (5) | 0.05 | 0.90 |
| | *Spectrally predicted variables* | | | |
| $P_{rem}$ | $P_{rem} = 20.79 + 1.285\ pH_{water} - 0.290\ C - 0.007\ Kt - 0.029\ Gb_{cbd} - 0.105\ Fe_2O_{3cbd} + 0.020\ S$ | (6) | 0.50 | 6.61 |
| | $P_{rem} = 24.897 - 0.261\ C - 0.027\ Gb - 0.099\ Fe_2O_{3cbd} + 0.019\ S$ | (7) | 0.49 | 6.72 |
| | $P_{rem} = 24.160 - 0.030\ Gb - 0.111\ Fe_2O_{3cbd} + 0.015\ S$ | (8) | 0.43 | 7.09 |
| $P_{resin}$ | $P_{res} = 0.847 + 0.058\ C - 0.001\ Kt - 0.001\ Gb - 0.007\ Fe_2O_{3cbd}$ | (9) | 0.41 | 0.71 |
| | $P_{res} = 1.777 - 0.002\ Kt - 0.002\ Gb - 0.007\ Fe_2O_{3cbd}$ | (10) | 0.20 | 0.84 |

$P_{rem}$: phosphorus remaining in solution; $P_{resin}$: phosphorus available; C: carbon; Kt: kaolinite estimated after extraction with sulfuric acid; Gb: gibbsite estimated after extraction with sulfuric acid; $Fe_2O_{3cbd}$: amount of Fe determined by the CBD method; S: sand; $R^2{}_c$: coefficient of determination of calibration; RMSE: root mean square error.
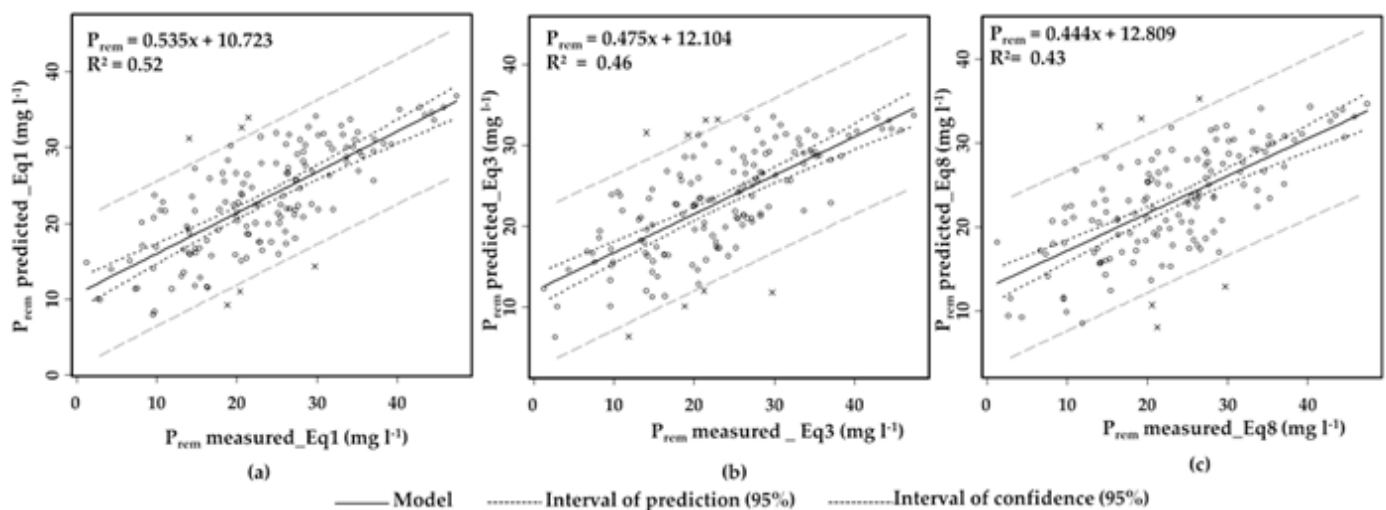


**Figure 2.** Relationships between the measured and predicted data, corresponding to the whole data set (148 samples), i.e., both the calibration and validation sets, using the best-fit pedotransfert function (Equation (1), (**a**)), a simplified function without C and pH (Equation (3), (**b**)), a simplified function without C and pH (Equation (8), (**c**)). Spectrally predicted variables were predicted by NIR/mPLS for $Fe_2O_{3cbd}$, MIR/mPLS for C and S, and by NIR according to Ramaroson et al. [24] for Kt and Gb. Large and narrow dashed lines are the confidence and prediction intervals, respectively; the circles and crosses are the points inside and outside the confidence interval.

We tested the same multiple regression analyses using the variables predicted with the PLS methods (carbon, $Fe_2O_{3cbd}$, sand) and with the NIR models proposed by Ramaroson et al. [25] for kaolinite and gibbsite. For $pH_{water}$, we used measured values as it could not be predicted with spectral methods. For $P_{rem}$, the multiple regression equations were approximately of the same quality as those obtained with only the measured variables (Equations (7) and (8) in Table 5; Figure 2c). Moreover, the relationship between $P_{rem}$ predicted using chemically measured data (Equation (3)) and $P_{rem}$ predicted with PTF using spectrally predicted data (Equation (8)) was good (slope = 0.83; $R^2$ = 0.74) (Figure 3).
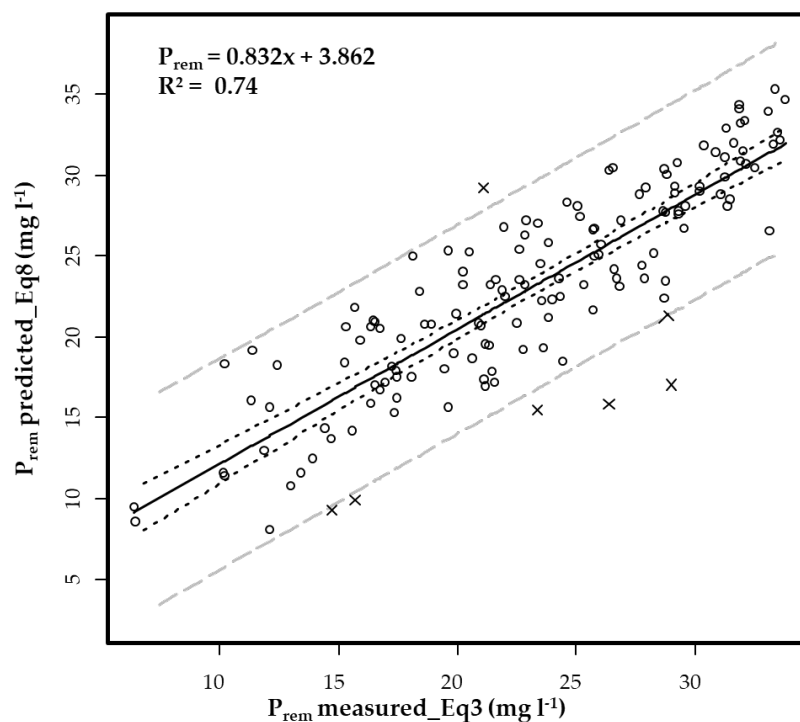
**Figure 3.** Relationships between the $P_{rem}$ predicted with PTF using chemically measured data (Equation (3)) and PTF using spectrally predicted data (Equation (8)). Spectrally predicted variables were predicted by NIR/mPLS for $Fe_2O_{3cbd}$, MIR/mPLS for S, and by NIR according to Ramaroson et al. [24] for Gb. Large and narrow dashed lines are the confidence and prediction intervals, respectively; the circles and crosses are the points inside and outside the confidence interval.

## 4. Discussion

### 4.1. Use of Infrared Spectroscopy to Develop P Availability Indices with Chemometric Methods

Phosphorus is an essential nutrient required by crops in large amounts. Soil testing is one of the most cost-effective nutrient management tools available to farmers and crop advisers. Soil tests provide an index of the labile plant-available P by extracting a fraction of the P that is related to the yield response of crops [37]. However, these indexes often fail to satisfactorily predict P availability [6,7].

Soriano-Disla et al. [18] have reviewed the performance of visible, near-, and mid-infrared reflectance spectroscopy for the prediction of soil physical, chemical, and biological properties using multivariate chemometric regression modeling. For P availability indices, with few exceptions of soil sets representing special or unusual conditions, most predictions of extractable P in soils resulted either in low $R^2_v$ values (0.5–0.7) or were considered to be completely unreliable ($R^2 < 0.50$). At regional or country scales, most of the results are unreliable with both NIR [24,30] and MIR [20,22,38]. An exception was reported by Morón and Cozzolino [39] who found low accuracy prediction, using NIR, for resin and Bray extractable P ($R^2_v = 0.61$ and $0.58$, respectively) for soils from Uruguay. Our results, presenting even lower coefficients ($R^2_v = 0.06$ for NIR and $0.36$ for MIR), are comparable to the majority of studies conducted on a similar scale.

Sorption of P in the soil controls its chemical mobility and bioavailability [40]. The ability of soil to bind phosphorus (P sorption) can be also a useful index of P availability. Good predictions were reported in the study of Soriano-Disla et al. [18] for P sorption with MIR (moderately successful predictions, median $R^2_v = 0.83$). However, the number of studies and geographic area studied (i.e., west Australia) are very limited [20,22,41]. Dunne et al. [21] also showed moderately successful predictions ($R^2_v$ up to 0.67) using different sorption models, i.e., single point sorption index, Langmuir sorption isotherm, and Freundlich sorption isotherm, the P sorption index determined as the P remaining in solu-

tion being the most successful. Studies using vis-NIR were less successful ($R^2_v$ = 0.69) [42]. Our results showed nearly the same accuracy of prediction, with $R^2_v$ = 0.65 and 0.77 for NIR and MIR, respectively, as the reported studies. However, these predictions could be used as acceptable soil quality indices for evaluating soil quality or fertility by African farmers who have no access to soil analysis due to high prices.

*4.2. Use of PTF to Relate P Availability Indices to Soil Properties*

The extent to which a soil adsorbs P (sorption capacity) differs widely among different soils. Factors controlling phosphate binding in soils have been the focus of research efforts in recent decades (e.g., [3,43]). P sorption tends to be high in soils with a high proportion of small-size particles such as clay and, hence, high specific surface area [43]. Aluminum and iron oxides are considered the main phosphate adsorbents in soils ([3] and references therein). Accordingly, close relationships were found between the amounts of adsorbed phosphate and certain aluminum and iron forms (crystalline and amorphous), which lead to the creation of pedotransfer functions for predicting adsorbed phosphate [23]. Crystalline Fe and Al oxides generally provide a large part of the P sorption capacity of highly weathered soils [44], while amorphous Fe and Al oxides contribute to the sorption of P by less weathered soils [23]. However, the amount of amorphous oxides is low with regards to crystalline ones, and, to our knowledge, it is not possible to quantify them independently by NIR or MIR. A substantial contribution of kaolinite to phosphate sorption has been also demonstrated recently [3]. The effect of pH and organic matter on phosphate sorption by clay minerals and Fe/Al oxides has been also extensively studied [35,45]. Briefly, soluble humic molecules and organic acids can be sorbed to Al and Fe oxide surfaces consequently blocking P adsorption sites, then decreasing P sorption and increasing P availability.

Chemical properties that are related to the mineral and organic components can be predicted spectrometrically because of the interaction between the soil properties and the active soil components: organic matter, clay minerals, and oxides [46]. Therefore, adsorption-desorption reactions, such as P availability or P sorption, can be predicted if quantitative mineralogy and chemical analysis of various properties are available. However, detailed mineralogical measurements and some specific analyses are expensive and rarely made in soil surveys. There exist a few PTFs that relate P sorption to aluminum and iron oxide contents [23]. Our results showed that, in addition to Fe/Al oxides, sand and carbon content are key parameters. These compounds have been predicted with a relatively good accuracy [18]. Demattê et al. [47] and Vendrame et al. [24] demonstrated the use of NIR spectroscopy for identifying major soil mineralogy in tropical soils from Brazil. Numerous studies have reported accurate predictions of soil total C and N content (e.g., [16,48,49]). Accurate calibration for sand using MIR or combined vis-NIR has been found, with $R^2_v$ between 0.70 and 0.99 [24,30,38,50,51].

Our results are in the range of most published results with reliable spectroscopy-based soil analysis for soil compounds used in our PTF, with $R^2_v$ of 0.87 for C (with MIR and PLS calibration); 0.76 for sand (MIR-PLS); 0.72 for $Fe_2O_{3cbd}$ (MIR-PLS); and 0.75 for gibbsite (NIR, height of the first derivative of specific peak at 2265 nm) (Table 3 and Figure 2.). The fit of multiple regression analyses for $P_{rem}$ or $P_{resin}$, using data obtained by chemical analyses and predicted values through spectrometry, were similar (Table 5), and a good relationship between the PTFs obtained by the two approaches was shown for $P_{rem}$ (Figure 3).

## 5. Conclusions

Highly weathered soils cover large areas in the tropics. The reactive minerals, i.e., clay minerals (kaolinite) and Al/Fe oxides (gibbsite, goethite, hematite), play a key role, together with organic matter, in the physico-chemical functioning of these soils, especially on P sorption. To overcome the widespread P deficiency in the agricultural soils of Sub-Saharan Africa and promote adequate soil P management, rapid and low-cost soil testing for P availability or P sorption capacity is needed. While numerous studies have been conducted to quantify the soil organic matter with infrared spectral methods (see [18]), research on

the prediction of P sorption capacity or P availability in soils using this approach is still scarce. Although these methods are ineffective in predicting available P ($P_{resin}$), we showed that reliable spectroscopy-based analyses of a P sorption index ($P_{rem}$) can be obtained with both NIR and MIR spectrometry using mPLS. The development of pedotransfer functions (PTFs) based on carbon content, texture, and mineralogical properties of soils predicted with chemometric methods is also useful for predicting $P_{rem}$ and through that in the understanding of the effects of the most important soil components controlling P sorption. Therefore, the P sorption capacity of the soil can be predicted based on the amounts of aluminum and iron oxides (gibbsite and $Fe_2O_{3cbd}$), which both increase P sorption, and the amount of sand, that counteract the effects of Fe/Al oxides. These soil components are fairly well predicted by IR-spectrometry, and a rapid and low-cost procedure for the estimation of P sorption capacity can be proposed. As farmers generally do not have access to soil testing in less developed countries (e.g., Madagascar), due to their cost and to the lack of routine laboratories, indices related to the P sorption potential of soils could be linked to cartographic data of the soils (i.e., mineralogy, C content) to improve fertilizers management. The hereby presented models represent encouraging results and foresee the need for similar studies on tropical soils in different environments to improve the method.

## References

1. Raminoarison, M.; Razafimbelo, T.; Rakotoson, T.; Becquer, T.; Blanchart, E.; Trap, J. Multiple-nutrient limitation of upland rainfed rice in ferralsols: A greenhouse nutrient-omission trial. *J. Plant Nutr.* **2020**, *43*, 270–284. [CrossRef]
2. Frossard, E.; Brossard, M.; Hedley, M.J.; Metherell, A. Reactions controlling the cycling of P in soils. In *Phosporus in the Global Environment: Transfers, Cycles and Management*; Tiessen, H., Ed.; John Wiley: Chichester, UK, 1995; pp. 107–137.
3. Gérard, F. Clay minerals, iron/aluminum oxides, and their contribution to phosphate sorption in soils—A myth revisited. *Geoderma* **2016**, *262*, 213–226. [CrossRef]
4. Cordell, D.; Drangert, J.O.; White, S. The story of phosphorus: Global food security and food for thought. *Glob. Environ. Chang.* **2009**, *19*, 292–305. [CrossRef]
5. Ulrich, A.E.; Frossard, E. On the history of a reoccurring concept: Phosphorus scarcity. *Sci. Total Environ.* **2014**, *490*, 694–707. [CrossRef]
6. Van Raij, B. Bioavailable tests: Alternatives to standard soil extractions. *Commun. Soil Sci. Plant Anal.* **1998**, *29*, 1553–1570. [CrossRef]
7. Zehetner, F.; Wuenscher, R.; Peticzka, R.; Unterfrauner, H. Correlation of extractable soil phosphorus (P) with plant P uptake: 14 extraction methods applied to 50 agricultural soils from Central Europe. *Plant Soil Environ.* **2018**, *64*, 192–201. [CrossRef]
8. Morel, C.; Fardeau, J.C. Le phosphore assimilable des sols intertropicaux: Ses relations avec le phosphore extrait par deux méthodes chimiques. *Agron. Trop.* **1987**, *42*, 248–257.
9. McGechan, M.B. Sorption of phosphorus by soil, part 2: Measurement methods, results and model parameter values. *Biosyst. Eng.* **2002**, *82*, 115–130. [CrossRef]
10. Barrow, N.J. The description of phosphate adsorption curves. *J. Soil Sci.* **1978**, *29*, 447–462. [CrossRef]

11. Ozanne, P.G. Phosphate nutrition of plants—A general treatise. In *The Role of Phosphorus in Agriculture*; Khasawneh, F.F., Sample, E.C., Kamprath, E.J., Eds.; American Society of Agronomy, Crop Science Society of America, Soil Science Society of America: Madison, WI, USA, 1980; pp. 559–589.

12. Bolland, M.D.A.; Gilkes, R.J.; Brennan, R.F.; Allen, D.G. Comparison of seven phosphorus sorption indices. *Soil Res.* **1996**, *34*, 81–89. [CrossRef]

13. Burkitt, L.L.; Gourley, C.J.P.; Hannah, M.C.; Sale, P.W.G. Assessing alternative approaches to predicting soil phosphorus sorption. *Soil Use Manag.* **2006**, *22*, 325–333. [CrossRef]

14. Burkitt, L.L.; Moody, P.W.; Gourley, C.J.P.; Hannah, M.C. A simple phosphorus buffering index for Australian soils. *Soil Res.* **2002**, *40*, 497–513. [CrossRef]

15. Alves, M.E.; Lavorenti, A. Remaining phosphorus and sodium fluoride pH in soils with different clay contents and clay mineralogies. *Pesqui. Agropecu. Bras.* **2004**, *39*, 241–246. [CrossRef]

16. Viscarra Rossel, R.A.; Walvoort, D.J.J.; McBratney, A.B.; Janik, L.J.; Skjemstad, J.O. Visible, near infrared, mid infrared or combined diffuse reflectance spectroscopy for simultaneous assessment of various soil properties. *Geoderma* **2006**, *131*, 59–75. [CrossRef]

17. Cécillon, L.; Barthès, B.G.; Gomez, C.; Ertlen, D.; Génot, V.; Hedde, M.; Brun, J.J. Assessment and monitoring of soil quality using near-infrared reflectance spectroscopy (NIRS). *Eur. J. Soil Sci.* **2009**, *60*, 770–784. [CrossRef]

18. Soriano-Disla, J.M.; Janik, L.J.; Viscarra Rossel, R.A.; MacDonald, L.M.; McLaughlin, M.J. The Performance of visible, near-, and mid-infrared reflectance spectroscopy for prediction of soil physical, chemical, and biological properties. *Appl. Spectrosc. Rev.* **2014**, *49*, 139–186. [CrossRef]

19. Kruse, J.; Abraham, M.; Amelung, W.; Baum, C.; Bol, R.; Kühn, O.; Lewandowski, H.; Niederberger, J.; Oelmann, Y.; Rüger, C.; et al. Innovative methods in soil phosphorus research: A review. *J. Plant Nutr. Soil Sci.* **2015**, *178*, 43–88. [CrossRef]

20. Forrester, S.T.; Janik, L.J.; Soriano-Disla, J.M.; Mason, S.; Burkitt, L.; Moody, P.; McLaughlin, M.J. Use of handheld mid-infrared spectroscopy and partial least-squares regression for the prediction of the phosphorus buffering index in Australian soils. *Soil Res.* **2015**, *53*, 67–80. [CrossRef]

21. Dunne, K.S.; Holden, N.M.; O'Rourke, S.M.; Fenelon, A.; Daly, K. Prediction of phosphorus sorption indices and isotherm parameters in agricultural soils using mid-infrared spectroscopy. *Geoderma* **2020**, *358*, 113981. [CrossRef]

22. Minasny, B.; Tranter, G.; McBratney, A.B.; Brough, D.M.; Murphy, B.W. Regional transferability of mid-infrared diffuse reflectance spectroscopic prediction for soil chemical properties. *Geoderma* **2009**, *153*, 155–162. [CrossRef]

23. Borggaard, O.K.; Szilas, C.; Gimsing, A.L.; Rasmussen, L.H. Estimation of soil phosphate adsorption capacity by means of a pedotransfer function. *Geoderma* **2004**, *118*, 55–61. [CrossRef]

24. Vendrame, P.R.S.; Marchão, R.L.; Brunet, D.; Becquer, T. The potential of NIR spectroscopy to predict soil texture and mineralogy in Cerrado Latosols. *Eur. J. Soil Sci.* **2012**, *63*, 743–753. [CrossRef]

25. Ramaroson, V.H.; Becquer, T.; Sá, S.O.; Razafimahatratra, H.; Larvy Delarivière, J.; Blavet, D.; Vendrame, P.R.S.; Rabeharisoa, L.; Rakotondrazafy, A.F.M. Mineralogical analysis of ferralitic soils in Madagascar using NIR spectroscopy. *Catena* **2018**, *168*, 102–109. [CrossRef]

26. IUSS Working Group WRB. *World Reference Base for Soil Resources 2014: International Soil Classification System for Naming Soils and Creating Legends for Soil Maps*; World Soil Resources Reports 106; Food and Agriculture Organization of the United Nations: Rome, Italy, 2014.

27. Alvarez, V.D.; Novais, R.D.; Dias, L.E.; Oliveira, J.D. Determinação e uso do fósforo remanescente. *Bol. Inf. Soc. Bras. Cienc. Solo* **2000**, *25*, 27–34.

28. Mehra, O.P.; Jackson, M.L. Iron oxide removal from soils and clays by a dithionite-citrate system buffered with sodium bicarbonate. *Clays Clay Miner.* **1960**, *7*, 317–327. [CrossRef]

29. Reatto, A.; Bruand, A.; Martins, E.S.; Muller, F.; da Silva, E.M.; de Carvalho, O.A.; Brossard, M. Variation of the kaolinite and gibbsite content at regional and local scale in Latosols of the Brazilian Central Plateau. *C. R. Geosci.* **2008**, *340*, 741–748. [CrossRef]

30. Chang, C.W.; Laird, D.A.; Mausbach, M.J.; Hurburgh, C.R. Near-infrared reflectance spectroscopy–principal components regression analyses of soil properties. *Soil Sci. Soc. Am. J.* **2001**, *65*, 480–490. [CrossRef]

31. Malley, D.F.; Martin, P.D.; Ben-Dor, E. Application in analysis of soils. In *Near-Infrared Spectroscopy in Agriculture*; Roberts, C.A., Ed.; Agronomy Monograph 44; American Society of Agronomy, Crop Science Society of America, Soil Science Society of America: Madison, WI, USA, 2004; pp. 729–784.

32. Madeira, J.; Bedidi, A.; Pouget, M.; Cervelle, B.; Flay, N. Spectral (MIR) determination of kaolinite and gibbsite contents in lateritic soils. *C. R. Acad. Sci. Ser. II-A* **1995**, *321*, 119–127.

33. Grinand, C.; Rajaonarivo, A.; Bernoux, M.; Pajot, V.; Brossard, M.; Razafimbelo, T. Estimation des stocks de carbone dans les sols de Madagascar. *Etude Gest. Sols* **2009**, *16*, 23–34.

34. Rabeharisoa, L.; Razanakoto, O.R.; Razafimanantsoa, M.P.; Rakotoson, T.; Amery, F.; Smolders, E. Larger bioavailability of soil phosphorus for irrigated rice compared with rainfed rice in Madagascar: Results from a soil and plant survey. *Soil Use Manag.* **2012**, *28*, 448–456. [CrossRef]

35. Haynes, R.J.; Mokolobate, M.S. Amelioration of Al toxicity and P deficiency in acid soils by additions of organic residues: A critical review of the phenomenon and the mechanisms involved. *Nutr. Cycl. Agroecosyst.* **2001**, *59*, 47–63. [CrossRef]

36. Kaiser, K.; Guggenberger, G. Mineral surfaces and soil organic matter. *Eur. J. Soil Sci.* **2003**, *54*, 219–236. [CrossRef]

37. Fixen, P.E.; Grove, J.H. Testing soils for phosphorus. In *Soil Testing and Plant Analysis*; Westerman, R.L., Baird, J.V., Christensen, N.W., Fixen, P.E., Whitney, D.A., Eds.; Soil Science Society of America: Madison, WI, USA, 1990; pp. 141–180.

38. Shepherd, K.D.; Walsh, M.G. Development of reflectance spectral libraries for characterization of soil properties. *Soil Sci. Soc. Am. J.* **2002**, *66*, 988–998. [CrossRef]

39. Morón, A.; Cozzolino, D. Measurement of phosphorus in soils by near infrared reflectance spectroscopy: Effect of reference method on calibration. *Commun. Soil Sci. Plant Anal.* **2007**, *38*, 1965–1974. [CrossRef]

40. Hinsinger, P. Bioavailability of soil inorganic P in the rhizosphere as affected by root-induced chemical changes: A review. *Plant Soil* **2001**, *237*, 173–195. [CrossRef]

41. Janik, L.J.; Forrester, S.T.; Rawson, A. The prediction of soil chemical and physical properties from mid-infrared spectroscopy and combined partial least-squares regression and neural networks (PLS-NN) analysis. *Chemometr. Intell. Lab. Syst.* **2009**, *97*, 179–188. [CrossRef]

42. Cohen, M.; Mylavarapu, R.S.; Bogrekci, I.; Lee, W.S.; Clark, M.W. Reflectance spectroscopy for routine agronomic soil analyses. *Soil Sci.* **2007**, *172*, 469–485. [CrossRef]

43. McGechan, M.B.; Lewis, D.R. Sorption of phosphorus by soil, part 1: Principles, equations and models. *Biosyst. Eng.* **2002**, *82*, 1–24. [CrossRef]

44. Agbenin, J.O. Extractable iron and aluminum effects on phosphate sorption in a savanna Alfisol. *Soil Sci. Soc. Am. J.* **2003**, *67*, 589–595. [CrossRef]

45. Muljadi, D.; Posner, A.M.; Quirk, J.P. The mechanism of phosphate adsorption by kaolinite, gibbsite and pseudoboehmite. I. The isotherms and the effect of pH on adsorption. *J. Soil Sci.* **1966**, *17*, 212–229. [CrossRef]

46. Minasny, B.; Hartemink, A.E. Predicting soil properties in the tropics. *Earth Sci. Rev.* **2011**, *106*, 52–62. [CrossRef]

47. Demattê, J.A.M.; Sousa, A.A.; Alves, M.C.; Nanni, M.R.; Fiorio, P.R.; Campos, R.C. Determining soil water status and other soil characteristics by spectral proximal sensing. *Geoderma* **2006**, *135*, 179–195. [CrossRef]

48. Madari, B.E.; Reeves, J.B., III; Coelho, M.R.; Machado, P.L.O.A.; De-Polli, H.; Coelho, R.M.; Benites, V.M.; Souza, L.F.; McCarty, G.W. Mid- and near-infrared spectroscopic determination of carbon in a diverse set of soils from the Brazilian national soil collection. *Spectr. Lett.* **2005**, *38*, 721–740. [CrossRef]

49. Brunet, D.; Barthès, B.G.; Chotte, J.L.; Feller, C. Determination of carbon and nitrogen contents in Alfisols, Oxisols and Ultisols from Africa and Brazil using NIRS analysis: Effects of sample grinding and set heterogeneity. *Geoderma* **2007**, *139*, 106–117. [CrossRef]

50. Morón, A.; Cozzolino, D. Exploring the use of near infrared reflectance spectroscopy to study physical properties and microelements in soils. *J. Near Infrared Spectrosc.* **2003**, *11*, 145–154. [CrossRef]

51. Madari, B.E.; Reeves, J.B., III; Machado, P.L.O.A.; Guimarães, C.M.; Torres, E.; McCarty, G.W. Mid-and near-infrared spectroscopic assessment of soil compositional parameters and structural indices in two Ferralsols. *Geoderma* **2006**, *136*, 245–259. [CrossRef]